Radiative Climatology of the North Slope of Alaska and the Adjacent Arctic Ocean

C. Marty, R. Storvold, and X. Xiong
Geophysical Institute
University of Alaska
Fairbanks, Alaska

K. H. Stamnes
Stevens Institute of Technology
Hoboken, New Jersey

B. D. Zak
Sandia National Laboratories
Albuquerque, New Mexico

Introduction

Recent climate modeling results point to the Arctic as a region that is particularly sensitive to global climate change (e.g., IPCC 1997). The North Slope of Alaska-Adjacent Arctic Ocean (NSA-AAO) Cloud and Radiation Testbed (CART) sites of the Atmospheric Radiation Measurement (ARM) Program are designed to collect data on temperature-ice-albedo and water vapor-cloud-radiation feedbacks are believed to be important to the predicted global warming (Stamnes et al. 1999). The main goals of the project are improving radiative transfer models in the Arctic environment and the testing of satellite remote sensing algorithms.

At the two NSA-AAO ARM sites, radiation data has now been collected through more than a complete annual cycle. Barrow is the main NSA-AAO site and represents the Arctic Ocean coastal climate whereas Atqasuk (100 km inland) on the other side is anticipated to have more continental character. What we present here is a preliminary investigation on one year (2000) of data of radiative fluxes and standard meteorological elements of these two sites and compare it with similar results obtained in the Arctic Ocean during the one-year (1997/98) Surface Heat Budget in the Arctic (SHEBA) Experiment. The radiative energy balance is calculated from upward and downward looking broadband radiometers. Albedo derived from broadband measurements is used to verify satellites derived albedo, which plays a key role for the determination of the radiation budget from space. Furthermore, we show the implementation and verification of a "Clear-Sky Index" (CSI), which can be used to distinguish between clear and cloudy sky at remote sites where we would otherwise not be able to do so.

Radiation Fluxes

Shortwave (SW) and longwave (LW) broadband radiation fluxes on all three sites were measured with an Eppley Precision Spectral Pyranometer (PSP), respectively an Eppley Precision Infrared Radiometer (PIR). All instruments were ventilated with slightly preheated air to prevent frost on the domes. The PIRs were operated shaded on a solar tracker because the dome is not absolutely blocking the direct sun from the detector and because direct solar radiation causes a non-uniform solar heating of the PIR dome. The radiation fluxes are stored as 1-minute averages, which we used to derive daily mean values. Finally, to better show the seasonal cycle the daily mean values were smoothed by a 30-day moving average.

The available energy from the radiation budget is, at all three sites, strongly dominated by the albedo. Net radiation in Barrow shows positive values from the beginning of April to the end of September with a maximum of about 200 W m^{-2} at the end of June and the beginning of July (Figure 1). Values above 50 W m^{-2} can only be observed from the beginning of June to mid-September, i.e., according to the albedo from the beginning of the snowmelt to the beginning of the next permanent winter snow cover. Minimum values of net radiation (about -80 W m^{-2}) are observed during December and January when no SW radiation is available since the sun is below the horizon. Net LW radiation varies shows no seasonal cycle and varies normally between almost zero and -70 W m^{-2}. Few daily mean values between mid-January and April even show positive values of net LW radiation (up to about 30 W m^{-2}) due to a strong inversion (despite the everlasting wind) near the ground. Longwave downwelling radiation can vary between about 120 W m^{-2} in winter and almost 400 W m^{-2} in summer. The daily mean values of direct solar radiation indicate that most clear-sky days occurred from March until mid-April with a few exceptions in July, August, and September. The clear decrease of global radiation (maximum values almost 350 W m^{-2}) in the second half of the summer is caused by the dominating stratoform cloud cover during that time of the year.

The downward looking instruments in Atqasuk were unfortunately not available before June. Hence, no net fluxes could be calculated before that time. The available data show much higher net radiation during early summer (maximum 300 W m^{-2}) in Atqasuk than in Barrow (Figure 2). This is mainly caused by about 50 W m^{-2} more daily global radiation (maximum 450 W m^{-2}), which is even enhanced by a slightly lower albedo in Atqasuk than in Barrow. The higher direct solar radiation in Atqasuk indicates that the higher global radiation is caused by less (or thinner) summer cloud cover in Atqasuk than in Barrow. This is confirmed by the comparison of the temperature normalized LW downwelling radiation (Figure 3) of the two sites. The LW downwelling radiation itself is very similar at the two sites despite the less cloud cover in Atqasuk because the mean temperature (Figure 4) in summer is quite higher in Atqasuk than in Barrow. The absolute humidity (Figure 5) is too low at both sites to cause a significant difference in the atmospheric radiation. The normalized LW downwelling radiation can therefore be used as an indicator for cloud cover at these two sites. The winter comparison of the normalized LW downwelling radiation indicates more cloud cover situations in Atqasuk than in Barrow and vice versa in summer. These results could be confirmed by a study, which used light detection and ranging (LIDAR) measurements in Atqasuk and Barrow to derive cloud cover at the two stations (Storvold et al. 2001). In winter (in absence of the sun) the larger number of clear-sky situations is

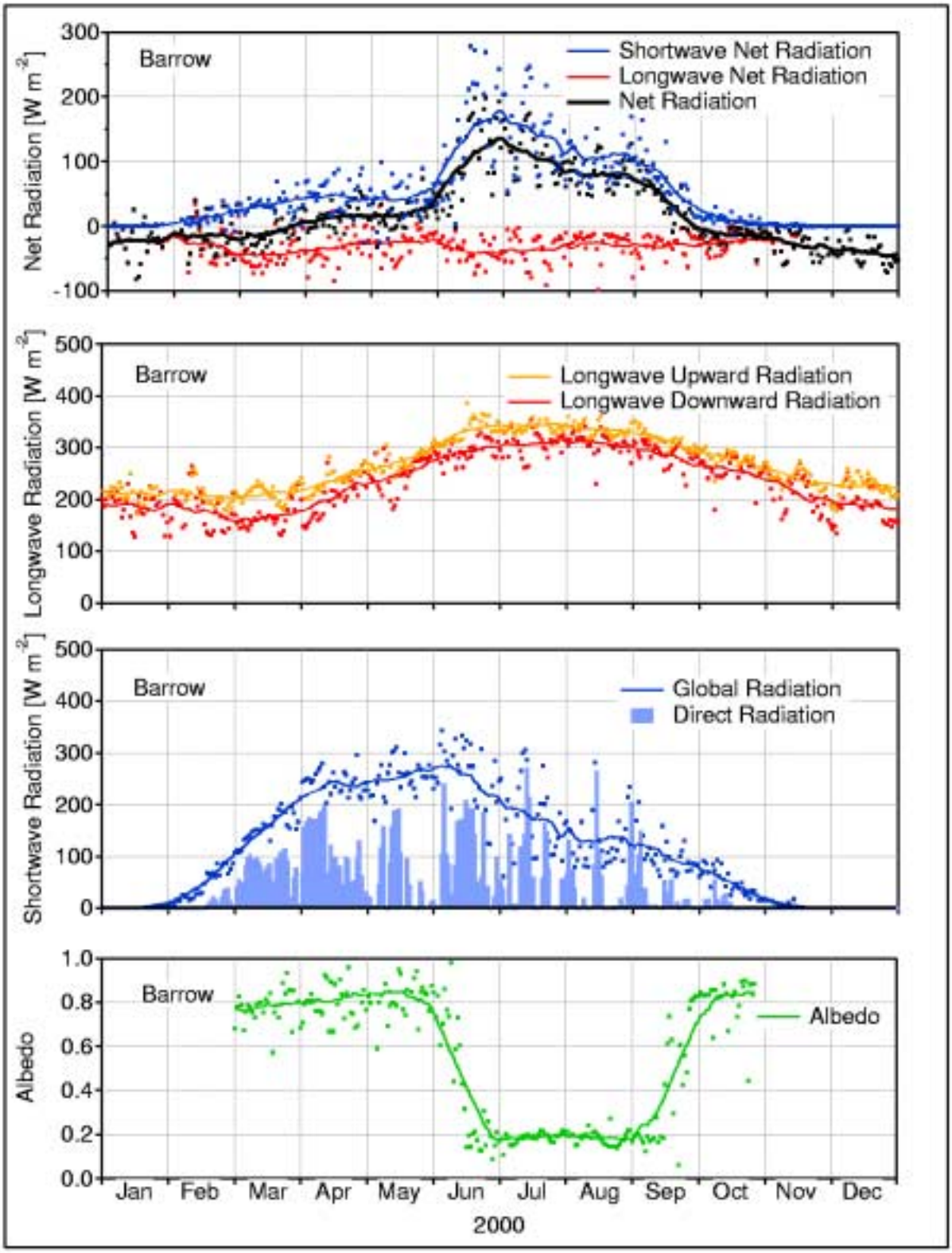

Figure 1. Annual cycle of the different radiation fluxes at Barrow during the year 2000.

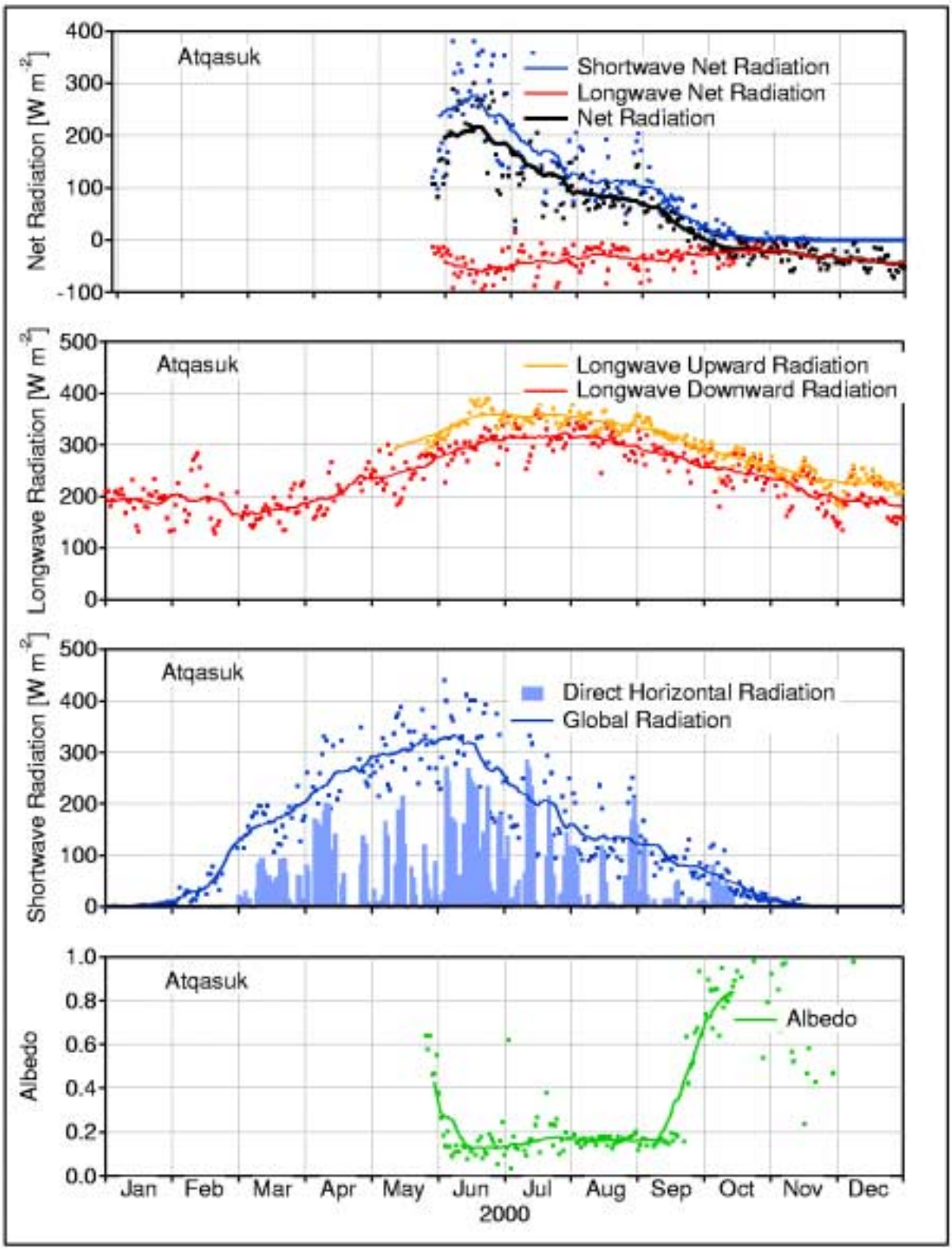

Figure 2. Annual cycle of the different radiation fluxes at Atqasuk during the year 2000.

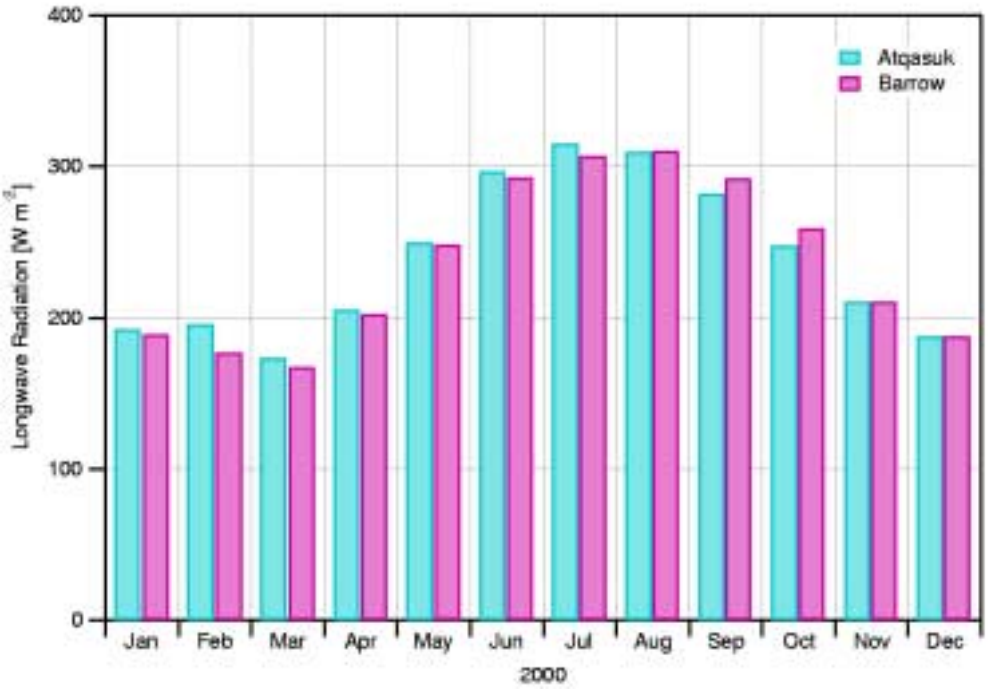

Figure 3. Temperature normalized LW downwelling radiation in Barrow and Atqasuk during the year 2000.

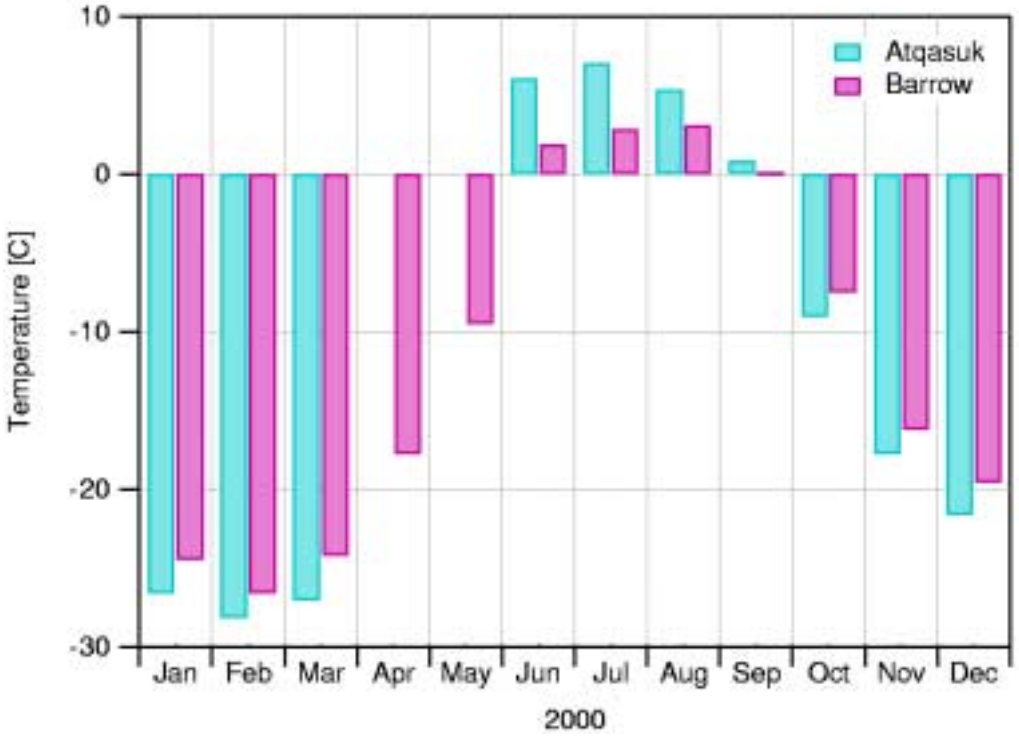

Figure 4. Air temperature in Barrow and Atqasuk during the year 2000.

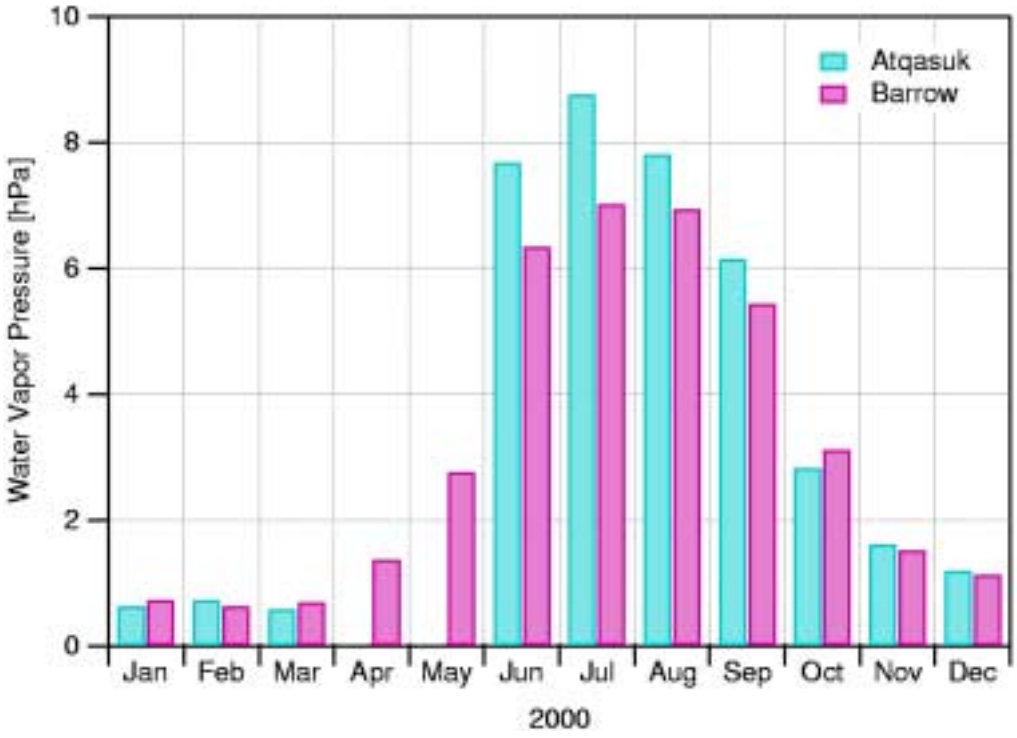

Figure 5. Water vapor (WV) pressure in Barrow and Atqasuk during the year 2000.

responsible for the lower air temperatures in Atqasuk than in Barrow. The warmer summer temperatures in Atqasuk cause an earlier snowmelt (about beginning of June), which according to the albedo values is about ten days earlier than in Barrow.

The SHEBA site was operational from October 1997 to September 1998 on a multi-year ice floe in the Arctic Ocean about 800 km north of Barrow. Despite the time and local differences of SHEBA to the two others sites some similarities and differences are worth to be compared. The seasonal cycle of net radiation (Figure 6) is not as pronounced due to the small change in the sea-ice albedo from winter (0.8) to summer (0.6). In contrast to Barrow, daily mean values of LW net radiation at the SHEBA site hardly got positive. Longwave downwelling radiation shows similar minimum values (about 120 W m^{-2}) in winter, whereas the maximum values in summer only reach a little bit more than 300 W m^{-2}. The smaller direct radiation values indicate that the high global radiation is mainly caused by multiple reflection between the sea-ice and low-level clouds.

Verification of Satellite Derived Albedo

Surface albedo is one of the most important factors influencing the radiation budget of the earth-atmosphere system. The Arctic surface albedo is characterized by a rapid and significant change of surface physical conditions during the short melt season. NSA-AAO data from Barrow was used to compare satellite-derived albedo during spring and summer 2000.

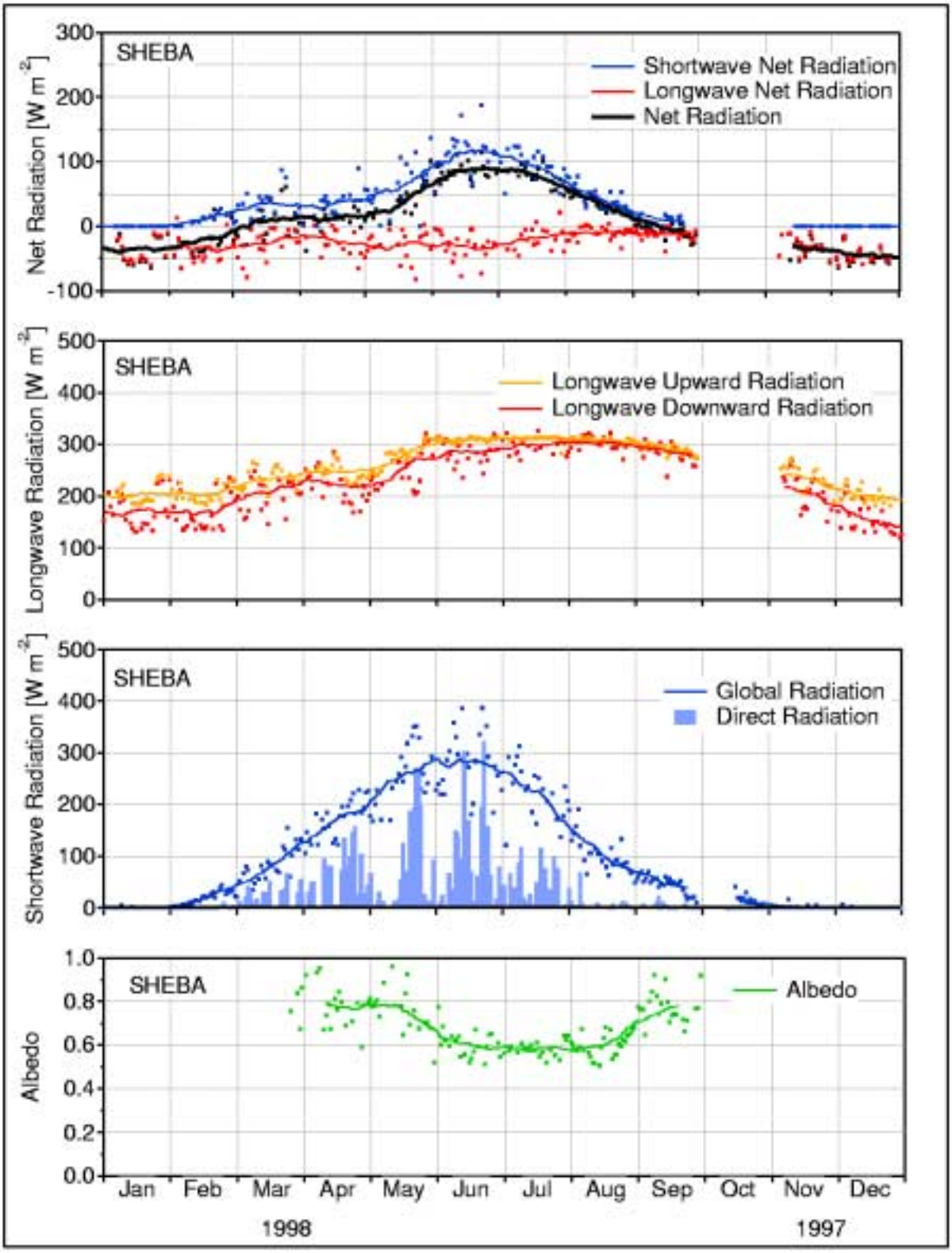

Figure 6. Annual cycle of the different radiation fluxes at SHEBA during the year 2000.

Advanced Very High Resolution Radiometer (AVHRR) data from the National Oceanic and Atmospheric Administration (NOAA) polar orbiting satellites were used to retrieve broadband albedo from space using channel 1 (visible) and channel 2 (near infrared) and applying narrow-to-broadband conversion (Xiong and Stamnes 2001). To improve accuracy only clear-sky near overhead passes with solar zenith angle < 70 were used.

The following comparison (Figure 7) between the satellite-derived albedo and the measured surface albedo (derived using daily mean up- and downwelling values) show encouraging good results for spring and first half of summer.

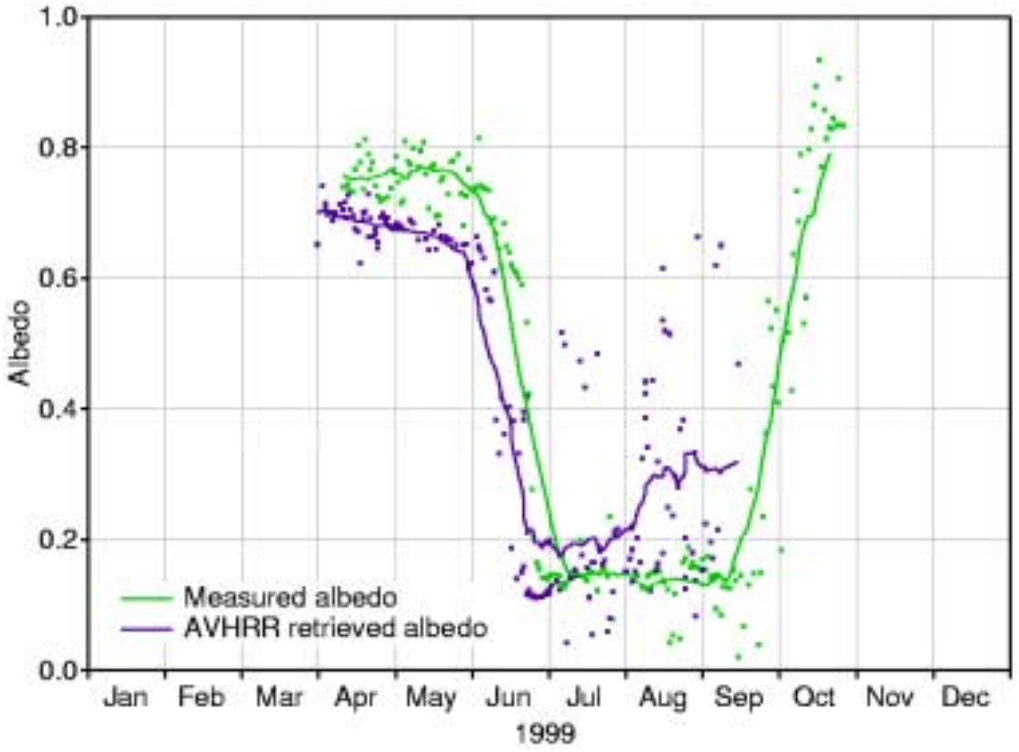

Figure 7. Measured and satellite-retrieved surface albedo during the year 1999 in Barrow.

The 10 percent lower satellite-derived albedo in spring and during the melt period can be explained with the large AVHRR grid size, which also includes icy ponds and windblown ridges. Errors in the AVHRR albedo seem to increase in the second part of the summer. This might be due to the fact that an almost permanent stratoform cloud layer during this time prevents the measurement of the necessary number of clear-sky pixels.

Detection of Clear-Sky Situations

Detailed climatological analysis and many investigations on radiation data demand for the distinction between clear-sky and cloudy sky situations. Approaches used so far, are based on synoptic sky

observations or SW measurements. The first includes temporal miss-matches and subjectivity. The second is limited to daytime hours. Furthermore, these two as well as other methods need special instrumentation or observations.

Our approach (Marty and Philipona 2000) uses LW downwelling radiation LW_d and the standard meteorological elements, air temperature T_a and humidity (water vapor pressure) e_a.

The method is based on the idea to continuously compare the measured apparent emissivity ε_A with the calculated theoretical clear-sky apparent emissivity ε_{AC} at the same moment. Whereas

$$\varepsilon_A = LW_d / \sigma T_a^4$$

ε_{AC} is calculated with an empirical formula, which uses measured T_a and e_a. A CSI can thus be defined:

$$CSI = \varepsilon_A / \varepsilon_{AC}, \; CSI \leq 1 \text{ clear-sky}, \; CSI > \text{cloud sky or overcast}$$

Figure 8 shows hourly values of CSI- and LIDAR-detected clouds during March 2000 at the ARM site at Barrow. Since the LIDAR is looking only at a small fraction of the sky straight above the instrument, the neighboring hourly values were included in the determination between clear and cloudy sky. The intercomparison generally shows good agreement between CSI and LIDAR. Some uncertainties might be explained with temporal and field-of-view differences between the two methods.

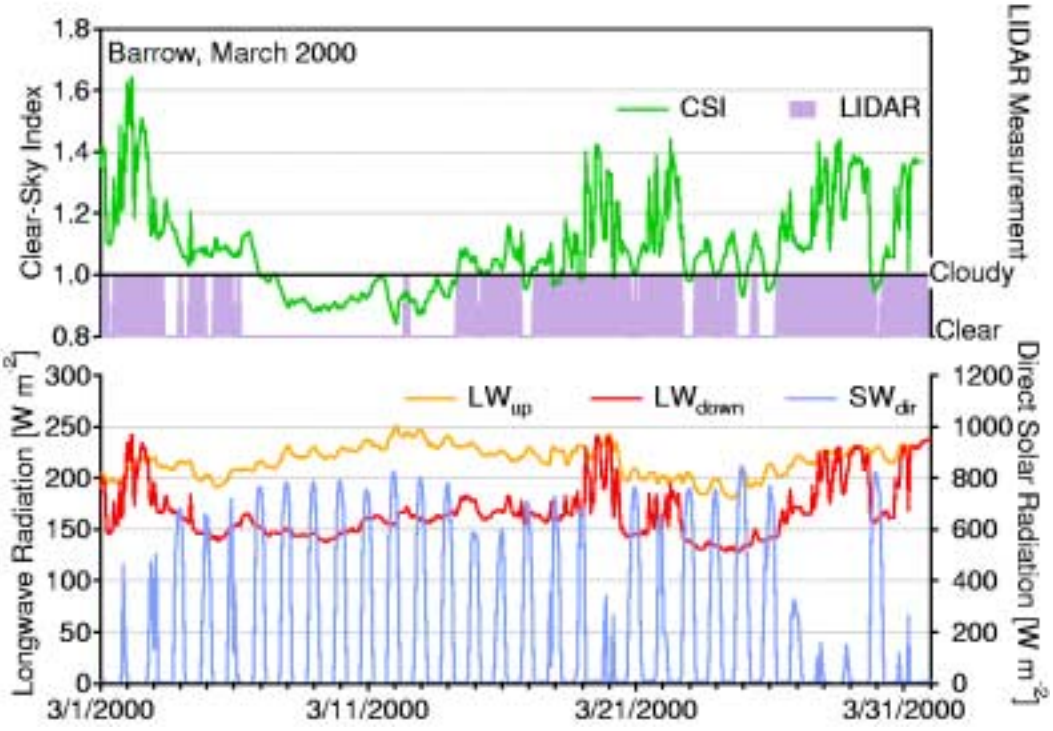

Figure 8. Intercomparison between the CSI and LIDAR measurements during March 2000 in Barrow.

Conclusions

Although Atqasuk is only about 100 km inland of Barrow and no topography is in between the two sites, the presented results demonstrate that Atqasuk experiences a somewhat more continental climate than Barrow, at least during the first year (2000) of measurements. Hence, Atqasuk shows a colder winter, but a warmer summer. An investigation of the temperature normalized LW downwelling radiation indicates that the different temperature regime might partly be driven by the seasonally different cloud cover in Atqasuk and Barrow. The higher number of spring cloudy sky situation would also explain the measured earlier snowmelt (and hence the earlier decrease in albedo) in Atqasuk compared with Barrow.

The satellite-derived albedo revealed on the one hand that stations like Barrow, Atqasuk, or SHEBA are a necessary condition if we want to improve our ability to derive radiation fluxes from space. Otherwise limitations due to a lack of clear-sky during summer in this part of the planet were also shown but should be significantly reduced with the new generation of space borne instruments.

The CSI algorithm applied to the Barrow data demonstrated that it is possible to continuously detect clear-sky situations with the help of LW atmospheric radiation and standard meteorological elements. The independency from solar radiation measurements makes this method very suitable for clear-sky detection during Arctic winter.

Acknowledgements

Data gaps in Barrow could partially be filled with data from the nearby NOAA Climate Monitoring and Diagnostics Laboratory station. San Diego State University kindly provided us with meteorological data of their field experiment in Atqasuk, what allowed us to fill some of our data gaps in Atqasuk.

Corresponding Author

C. Marty, chris@gi.alaska.edu, (907) 474-7360

References

IPCC Special Report (R. T. Watson, M. C. Zinyowera, and R. H. Moss), 1997: The regional impacts of climate change: An assessment of vulnerability, a special report of IPCC working group II, Cambridge University Press, United Kingdom.

Marty, C., and R. Philipona, 2000: The Clear-Sky Index to separate clear-sky from cloudy sky situations in climate research. *GRL*, **27**(17), 2649-2652.

Stamnes K., R. G. Ellingson, J. A. Curry, J. E. Walsh, and B. D. Zak, 1999: Review of science issues, deployment strategy, and status for the ARM North Slope of Alaska-Adjacent Arctic Ocean Climate Research site. *J. of Climate*, **12**, 46-63.

Storvold R., Ch. Marty, K. Stamnes, and B. D. Zak, 2001: Seasonal variability in cloud cover, cloud base height, and cloud liquid water content at the North Slope of Alaska and the Adjacent Arctic Ocean. This proceedings.

Xiong X., and K. Stamnes, 2001: Surface albedo over high Arctic Ocean derived from AVHRR and its validation with SHEBA data. *J. Appl. Meteorology*, submitted.